This full text paper was peer reviewed at the direction of IEEE Communications Society subject matter experts for publication in the IEEE ICC 2009 proceedings

# Measuring Indoor Mobile Wireless Link Quality

Andreas Wapf and Michael R. Souryal
Advanced Network Technologies Division
National Institute of Standards and Technology
Gaithersburg, Maryland, USA
andreas@wapf.ch, souryal@nist.gov

***Abstract*—This paper investigates methods for link quality measurement of an indoor, time-varying wireless link. Link quality estimates are used for a number of higher-layer functions, including rate adaptation, routing, and topology control. The objective is to rapidly and efficiently estimate the current reliability of an RF link in terms of its packet success probability in the presence of a time-varying channel. We compare various approaches to estimating the current packet success rate (PSR), including packet counting and several methods employing physical layer signal-to-noise ratio (SNR) measurements. Among the SNR-based estimators, we consider those using a simple moving average, an exponential moving average, and a Yule-Walker predictor of the current SNR. The analysis shows that the SNR-based estimators are more efficient than packet counting methods in terms of the number of measurements needed, are more accurate when link quality variability increases, and are more flexible in terms of predicting the PSR for various bit rates and packet sizes. An important requirement, however, of the SNR-based estimators is *a priori* knowledge of the SNR-PSR relationship, which is environment- and radio-dependent. An efficient methodology for obtaining this mapping is presented.**

## I. Introduction

Accurate and timely estimates of RF link quality are important to a number of higher layer functionalities in wireless networking, such as routing, rate adaptation and topology control. In multihop network routing protocols, recently proposed link metrics such as expected transmission count (ETX) [1], expected transmission time (ETT) [2], and the draft IEEE mesh networking standard's airtime link metric [3] all rely on some measure of link quality, usually the packet success rate over the link. In rate adaptation, the transmitter selects the maximum transmission data rate that can be sustained by the current quality of the link (e.g., [4]). In the area of topology control, link quality measures are used to determine when to hand over a mobile user to another cell or sector, or when to deploy relays in a multihop network that is created in real time [5].

The purpose of this paper is to evaluate the performance of various RF link quality estimation techniques on a time-varying digital wireless link. The quality of a link is measured, here, in terms of its reliability, defined as the probability that a packet is transmitted successfully. As the link quality varies with time, this probability is also a function of time and can be viewed as a random process. The objective of the estimator is to obtain an estimate of this probability at any given time.

We focus on two classes of estimators, packet counting and SNR-based. Packet counting (PC) estimators measure the packet success rate (PSR) directly by calculating the ratio of the number of successful packet transmissions to the total number of transmissions. Calculation of the ETX link metric, for example, was proposed to use a packet counting approach [1]. The advantages of PC-based estimators are that they are simple, intuitive, and require little or no *a priori* information. Their disadvantages are the accuracy, timeliness, and overhead of the measurements. The precision of PC-based estimates depends on the number of transmissions of the packets of interest. On the other hand, a large number of transmissions incurs a latency in the estimate, which can make it obsolete in time-varying conditions. Furthermore, since packet success rate, in general, depends on the size of the packet and the data rate (i.e., the modulation-coding scheme) at which packets are transmitted, PC-based estimates are specific to the bit rates and packet sizes of the counted packets. Some of these issues can be addressed through passive measurement of existing data traffic, active measurement using unicast transmissions, or some combination thereof (e.g., [6]).

SNR-based link quality estimators make use of SNR measurements obtained from the physical layer of the communications stack. They rely on the assumption that there is a strong correlation between the measured SNR and the current PSR of a link. The advantages of SNR-based estimators are that they potentially require fewer measurements, are more timely, and are more accurate than PC-based estimators in time-varying conditions. Their primary disadvantage is that they require prior information on the mapping between the SNR and PSR, which is environment- and radio-dependent.

Previous results on SNR-based link quality estimation are mixed. A thorough study of an outdoor, static IEEE 802.11b network concluded that the SNR reported by the physical layer is not predictive of link reliability [7]. However, the study also demonstrated that the multipath delays experienced outdoors far exceeded the delays tolerated by the radios that were used, generating significant intersymbol interference. A subsequent *indoor* study of a static 802.11 network operating at the 2 Mbps data rate showed a strong correlation between measured SNR and PSR, and one that follows the theoretical relationship quite closely, provided external interference is limited [8]. In [9], the authors showed an SNR-based estimator to converge more rapidly than a PC-based estimator on a link experiencing a sudden change in transmission power. This estimator maps Kalman-filtered SNR measurements to PSR using an empirical model. In other related work, [10] describes a hybrid approach using both SNR and packet counting to

classify links as "good" or "bad."

Our work differs from previous work in several respects. First, we emphasize performance in time-varying channels, which we induce through controlled, small-scale mobility. Second, we investigate estimator performance at multiple data rates and packet sizes. Third, our approach to SNR-based estimation mitigates the bias of using SNR measurements from only successfully received transmissions; it does so by employing measurement probes transmitted at a lower (and, hence, more reliable) data rate than that of the data packets of interest. We optimize the parameters of each estimator, and compare their performance over a range of channel variability speeds. The results suggest that SNR-based schemes have the potential to provide better and more efficient estimates of link reliability than PC-based schemes, especially as the time variability (or Doppler spread) of the channel increases.

Section II describes the estimators to be analyzed. Section III details the methodology used to collect experimental data. Section IV discusses trade-offs in the design of the estimators and proposes optimum parameters for each based on experimental results. The estimators are evaluated in Section V, and Section VI summarizes the conclusions.

## II. Proposed Estimators

The performance of four link quality estimators is analyzed: one packet-counting-based estimator and three SNR-based estimators. The SNR-based estimators differ in how they filter the raw SNR measurements generated by the receiver.

### A. Packet Counting

Packet counting refers to the estimation of link reliability by direct measurement of the ratio of successfully received packets to transmitted packets. If $w$ is the number of expected packets during an observation window, then the PC-based PSR estimate at time index $n$ is defined as

$$\hat{P}_{pc,n}(w) \triangleq \frac{I_{n-1} + I_{n-2} + \ldots + I_{n-w}}{w}$$

where $I_j$ is an indicator equal to one if the $j$th expected packet was successfully received, and zero otherwise.

Use of the PC-based estimator assumes that the receiver can learn of missing packets using, for example, either sequence numbers or knowledge of the rate at which packets are transmitted. The packets that are counted could be data packets generated by the application or special-purpose probing packets as in [1]. In practice, to support bidirectional estimation of a link, each end of the link can piggyback its measurement on its transmitted packets.

There exists a tradeoff in PC-based estimation between the increasing resolution of the PSR estimate and the associated increase in latency with increasing $w$. The increase in latency is of particular concern in time-varying channels. Another concern is the availability of packets, or the overhead of the probes (or test packets), needed to make an estimate.

A limitation of the PC-based approach is that the estimated PSR is applicable only to the size and data rate of the packets being counted. For example, a PSR estimate based on short broadcast packets transmitted at a low data rate may not be indicative of the PSR of longer data packets transmitted at a higher data rate. Nevertheless, PC-based schemes have been proposed and are in use in wireless implementations (e.g., [11]) because of their simplicity and portability.

### B. SNR-Based

SNR-based estimators are predicated on the notion that the probability of successful packet reception is a function of the signal-to-noise ratio at the receiver. These estimators first make an estimate of the SNR using measurements of the received signal energy and noise energy made available by the physical layer of the receiver. The SNR estimate is then mapped to a PSR estimate using a pre-defined function.

To account for noise in the radio's SNR measurements and to exploit any correlation that may be present in these measurements, we consider estimators that filter the radio's raw SNR measurements to predict the current SNR. Denoting the SNR measurement at time $n$ by $s_n$, $n \geq 0$, the filtering operation by $f(\cdot)$, and the SNR-PSR mapping by $g(\cdot)$, then the SNR and PSR estimates, respectively, at time $n$ are

$$\begin{aligned} \hat{s}_n &= f(s_0, s_1, \ldots, s_{n-1}) \\ \hat{P}_{f,n} &= g(\hat{s}_n). \end{aligned}$$

The SNR-PSR mapping function, $g(\cdot)$, may be based on a model of the equivalent discrete-input, discrete-output channel, if a suitable one is available, or it may be obtained empirically.

In the ensuing analysis, we consider three SNR filters, $f(\cdot)$: a simple moving average, an exponential moving average, and a Yule-Walker predictor.

*1) Simple Moving Average:* With the simple moving average (SMA), the current SNR estimate is the running sample mean of the SNR measurements observed during a prior interval. If the number of measurements during the observation window is $w$, then the SMA filter is defined for $n \geq w$ as

$$f_{\text{sma}}(w) \triangleq \frac{s_{n-1} + s_{n-2} + \ldots + s_{n-w}}{w}.$$

*2) Exponential Moving Average:* While the SMA gives equal weight to a finite number of measurements, the exponential moving average (EMA) gives greater weight to more recent observations and exponentially decreasing weight to older observations. The rate of decrease is governed by a smoothing factor, $\alpha$, which ranges between 0 and 1. The EMA filter is defined for $n \geq 1$ as

$$f_{\text{ema}}(\alpha) \triangleq \alpha s_{n-1} + (1-\alpha)\hat{s}_{n-1}$$

with the initial condition being $\hat{s}_0 = 0$.

*3) Yule-Walker Predictor:* The Yule-Walker (YW) predictor attempts to exploit knowledge of the statistics of the SNR process in order to predict the current SNR. It is optimum in the sense that it minimizes the mean square error of the estimate, assuming the process is wide-sense stationary [12].

The YW predictor is a finite linear filter of length $w$,

$$f_{\text{yw}}(w) \triangleq \sum_{k=1}^{w} h_k s_{n-k}$$

Fig. 1. Transmitting radio on positioner

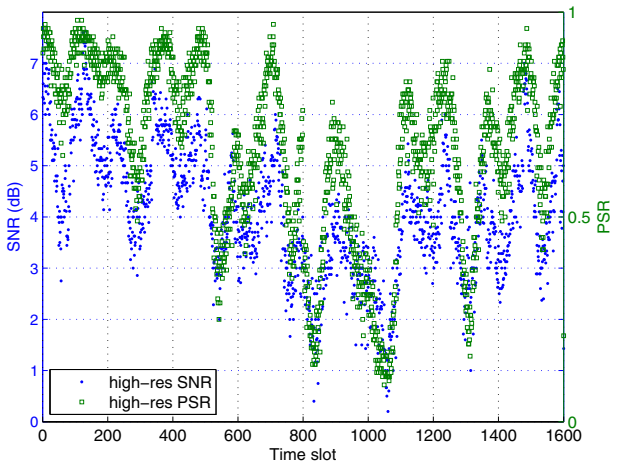


Fig. 2. High-resolution SNR and PSR vs. time, 5.5 Mbps data packets

where the filter coefficients, $h_k$, are given by

$$\begin{bmatrix} h_1 \\ h_2 \\ \vdots \\ h_w \end{bmatrix} = \begin{bmatrix} R_0 & R_1 & R_2 & \cdots & R_{w-1} \\ R_1 & R_0 & R_1 & \cdots & R_{w-2} \\ \vdots & \vdots & \vdots & \ddots & \vdots \\ R_{w-1} & \cdots & \cdots & R_1 & R_0 \end{bmatrix}^{-1} \begin{bmatrix} R_1 \\ R_2 \\ \vdots \\ R_w \end{bmatrix}$$

and where the autocorrelation function is $R_d = \mathrm{E}\left[s_m s_{m+d}\right]$, the statistical expectation of the product of two observations separated in time by $d$. A key difference between the YW filter and the two previous filters is its dependence on knowledge of the second-order statistics of the SNR process in the form of the autocorrelation function, $R_d$.

## III. Methodology

To evaluate the performance of the proposed estimators, we collected experimental data from a time-varying wireless link in an indoor environment. IEEE 802.11b/g radios were used at both ends of the link. Packet success/failure and SNR measurements were collected for non-line-of-sight propagation paths on a single floor of an office building. All other known 2.4 GHz 802.11 emitters in the building were shut off during these experiments.

To induce variability in the channel, a combination of controlled small-scale mobility and variable transmission power was used to generate fluctuations in the received signal strength. The transmitter was placed on a 50 cm linear positioner controlled by a programmable stepping motor (Fig. 1). The positioner moved the transmitter in steps of 0.62 mm. At each step, a batch of 100 data packets and 10 short broadcast packets was transmitted, with each packet containing a unique sequence number. Each data packet was transmitted without MAC layer retransmission and without RTS/CTS. Each broadcast packet was transmitted at 2 Mbps, and each data packet was transmitted at a given 802.11b/g data rate greater than 2 Mbps. The batch transmissions were repeated at each 0.62 mm step along the 50 cm span, equivalent to four wavelengths at the 2.4 GHz carrier and providing a measurement resolution of just over 200 measurements per wavelength. For a given data rate, measurements were collected for 3 sweeps of each of 3 different 50-cm spans, or 9 sweeps in total. On each span, the initial transmission power level was selected manually to target a PSR of approximately 50%, and the power level was automatically varied over a range of $\pm 3$ dB in increments of 1 dB every two wavelengths.

The stationary receiver recorded the number of received data packets and the DS/CDMA chip SNR of each received broadcast packet in each batch. The purpose of making SNR measurements using the lower-rate broadcast packets rather than the higher-rate data packets themselves was to mitigate the bias that results from only measuring the SNR of successfully received data packets, which is significant at low PSR. Since lower data rate transmissions are typically more reliable than higher data rate transmissions, SNR measurements can be received at a relatively high rate even when the data PSR is low.

The measurements of the number of received data packets and of SNR in each batch allow us to generate high-resolution estimates of the PSR and SNR at each step. Referring to each step duration as a time slot, Fig. 2 plots the high-resolution estimates versus time slot of one segment of data consisting of two sweeps of a 50 cm span. The data packets were transmitted at 5.5 Mbps with 64-byte payloads. Each high-resolution SNR estimate is averaged over the (up to) 10 SNR measurements that were made at each step. We observe in this segment a dynamic channel ranging in SNR from 0 to 8 dB and in PSR from 0 to 1.

Trace data like that shown in Fig. 2 can also be used to evaluate the performance of the various estimators. Our approach is to sub-sample (or decimate) the high-resolution data and input the sub-sampled data to the estimator. The degree to which we sub-sample (e.g., every tenth sample, every hundredth sample) dictates the effective speed of the time-varying channel as seen by the estimator. Furthermore, rather than use every available measurement (i.e., all 100 data packets or all 10 SNR measurements) at each step, the estimator, in practice, would only be able to collect one measurement per

step position. For example, a PC-based estimator would only receive an indication of whether a single packet was or was not successfully received at a given step. In our analysis, the estimator selects the single observation randomly (one of the 100 data packet transmissions, with equal probability). The performance of the estimators is then evaluated by comparing their estimates with the high-resolution estimates derived from *all* the available measurements at each step.

## IV. Estimator Design

The SNR-based estimators rely on a SNR-PSR mapping function, $g(\cdot)$, by which to obtain a PSR estimate. We describe our approach to obtaining this mapping and present the results. We also optimize the estimators over their parameter values (e.g., the window size $w$ of the PC-based estimator, the smoothing factor $\alpha$ of the EMA filter, etc.).

### A. SNR-PSR Mapping

One approach to obtaining the SNR-PSR mapping function is to model the transmitter-channel-receiver chain for the channel environment and modulation-coding scheme of interest. Such an explicit model can be difficult to obtain. Another approach is to build the mapping function empirically through direct observation, and this is the approach we have chosen.

Referring again to the SNR and PSR trace data in Fig. 2, there is clearly a correlation between the measured SNR and PSR, as they tend to rise and fall synchronously. Despite the seeming correlation, simple scatter plots of the high-resolution SNR versus PSR estimates—shown in Fig. 3 for three data rates (5.5, 24, and 54 Mbps) and 1518-byte payloads—do not reveal a well-defined mapping, especially in the transition region of moderate PSR. However, "boxplots" of the same data, shown in Fig. 4, grouped by integer values of the SNR (in dB), are more revealing. In the boxplot, the dividing line of the box is the median observed PSR value at that (rounded) SNR value, and the upper and lower parts of the box correspond to the upper and lower quartiles of the observations. The length of the box, or the interquartile range, contains 50% of the observations. Outliers, defined as observations lying above or below the box by 1.5 times the interquartile range, are denoted with $+$ markers.

Fig. 4 illustrates largely monotonic relationships between the SNR and the *median* PSR for all three data rates. Furthermore, the length of each box indicates the degree of uncertainty in the PSR value at that SNR. For the purpose of choosing a specific SNR-PSR mapping function, our SNR-based estimators map each SNR estimate to the median PSR, interpolating between adjacent median values for non-integer SNR estimates. An SNR-PSR mapping was obtained in this way for each of the 5.5, 24 and 54 Mbps data rates.

### B. Filter Parameters

Each estimator's filter, $f(\cdot)$, is characterized by the length of the filter or, in the case of the SNR-based EMA estimator, a smoothing factor. We select the filter lengths and smoothing factor that minimize an error metric. For the SNR-based

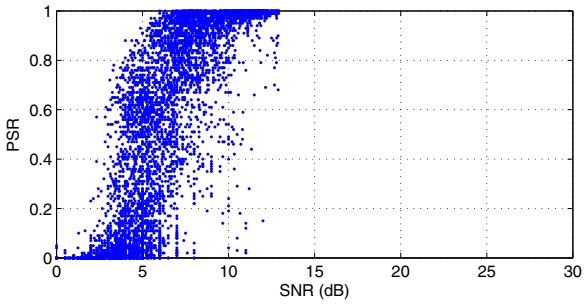


(a) 5.5 Mbps

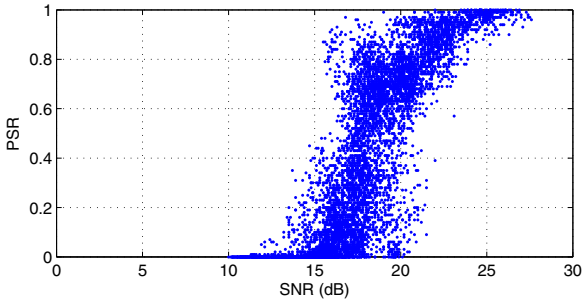


(b) 24 Mbps

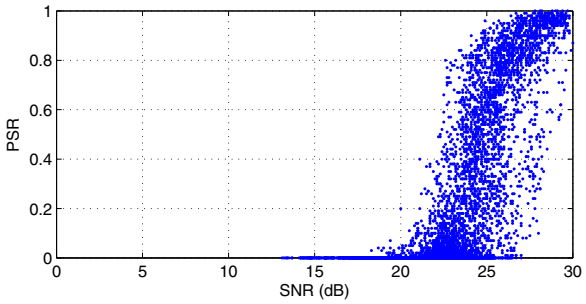


(c) 54 Mbps

Fig. 3. High-resolution PSR vs. SNR scatter plots

estimators, we minimize the median absolute error (in dB) in the SNR estimate, and for the PC-based estimator we minimize the median absolute error in the PSR estimate.[1] We choose to minimize the median absolute error rather than the mean square error in order to mitigate the impact of outliers, which appear to be non-negligible as seen in Fig. 4.

Fig. 5 plots the median absolute SNR estimation error of the three SNR-based estimator filters as a function of the filter length for SMA and YW, and as a function of the smoothing factor for EMA. These results are based on the superset of all our collected traces, consisting of 9 sweeps at each of the 5.5, 24 and 54 Mbps data rates. In the case of the YW predictor, the autocorrelation function is evaluated in advance using all available SNR samples, which should yield an upper bound on its performance. In each plot of Fig. 5, three cases of the sub-

[1]The SNR-based estimators could alternatively be designed to minimize the error in the PSR, rather than the SNR. We tried both and found there to be a negligible difference in ultimate performance between the two.

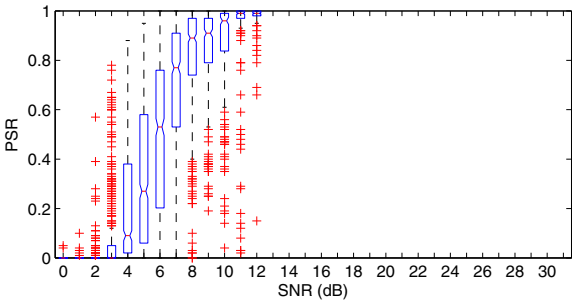


(a) 5.5 Mbps

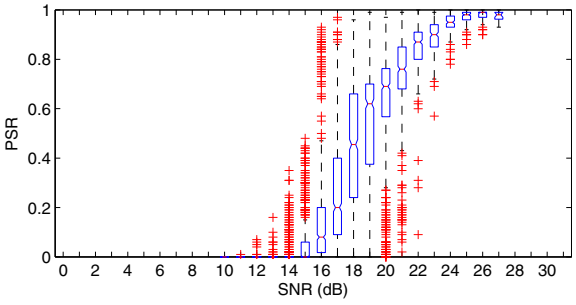


(b) 24 Mbps

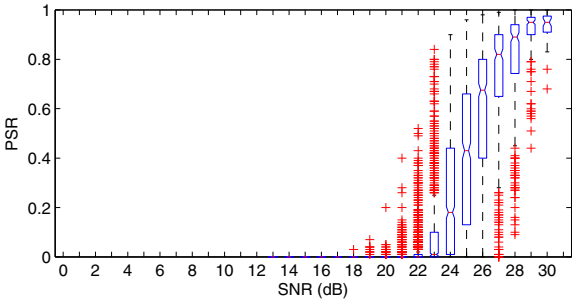


(c) 54 Mbps

Fig. 4. High-resolution PSR vs. SNR boxplots showing median, upper and lower quartiles, and outliers around integer values of the SNR estimates

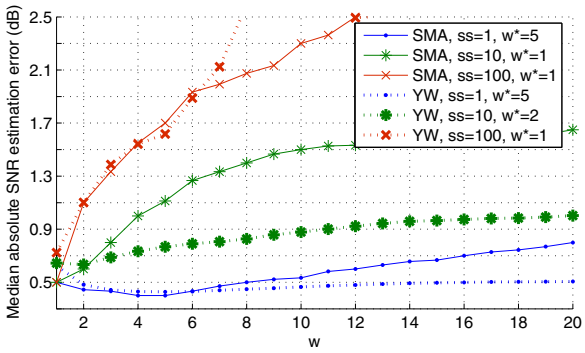


(a) Simple moving average and Yule-Walker filters

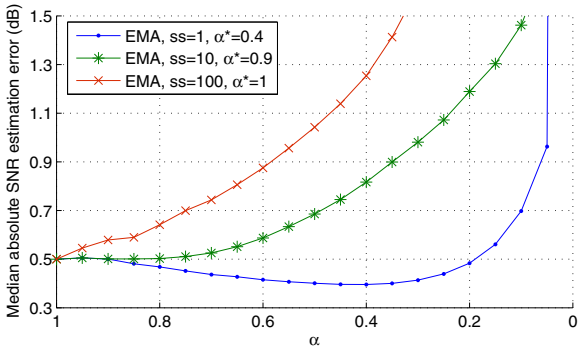


(b) Exponential moving average filter

Fig. 5. Median absolute estimation error vs. filter length ($w$)/smoothing factor ($\alpha$), by sub-sampling interval ($ss$)

| | | $ss=1$ | | | $ss=10$ | | | $ss=100$ | | |
|---|---|---|---|---|---|---|---|---|---|---|
| | | $\mu$ | $\tilde{x}$ | $\sigma$ | $\mu$ | $\tilde{x}$ | $\sigma$ | $\mu$ | $\tilde{x}$ | $\sigma$ |
| 5.5 Mbps | PC | 0.12 | 0.08 | 0.10 | 0.19 | 0.15 | 0.15 | 0.21 | 0.20 | 0.15 |
| | SMA | 0.20 | 0.14 | 0.19 | 0.23 | 0.16 | 0.22 | 0.18 | 0.12 | 0.18 |
| | EMA | 0.20 | 0.14 | 0.20 | 0.22 | 0.15 | 0.21 | 0.18 | 0.12 | 0.18 |
| | YW | 0.21 | 0.14 | 0.20 | 0.21 | 0.14 | 0.20 | 0.18 | 0.12 | 0.18 |
| 24 Mbps | PC | 0.12 | 0.09 | 0.10 | 0.18 | 0.15 | 0.15 | 0.20 | 0.14 | 0.18 |
| | SMA | 0.14 | 0.09 | 0.15 | 0.16 | 0.11 | 0.16 | 0.18 | 0.10 | 0.19 |
| | EMA | 0.15 | 0.09 | 0.15 | 0.16 | 0.11 | 0.15 | 0.18 | 0.10 | 0.19 |
| | YW | 0.15 | 0.09 | 0.15 | 0.16 | 0.11 | 0.15 | 0.18 | 0.11 | 0.19 |
| 54 Mbps | PC | 0.12 | 0.09 | 0.10 | 0.24 | 0.20 | 0.19 | 0.27 | 0.25 | 0.17 |
| | SMA | 0.17 | 0.11 | 0.17 | 0.18 | 0.13 | 0.17 | 0.21 | 0.16 | 0.20 |
| | EMA | 0.17 | 0.11 | 0.17 | 0.18 | 0.13 | 0.17 | 0.21 | 0.16 | 0.20 |
| | YW | 0.17 | 0.11 | 0.17 | 0.18 | 0.13 | 0.17 | 0.21 | 0.15 | 0.18 |

TABLE I
MEAN ($\mu$), MEDIAN ($\tilde{x}$), AND STANDARD DEVIATION ($\sigma$) OF THE PSR ESTIMATION ERROR BY CHANNEL SUB-SAMPLING ($ss$) AND DATA RATE

sampling interval are shown: (i) where every sample (step) of the high-resolution data is input to the estimator, (ii) every 10th sample, and (iii) every 100th sample. An increase in the sub-sampling interval (denoted by $ss$) translates to either a slower channel sampling rate or, equivalently, a faster time-varying channel. We observe that at the highest sampling rate ($ss = 1$), the optimum filter lengths are $w^*_{\text{sma}} = w^*_{\text{yw}} = 5$, and the optimum smoothing factor for EMA is $\alpha^* = 0.4$. At a lower sampling rate ($ss = 10$), the filters depend on less historical data, with $w^*_{\text{sma}} = 1$, $w^*_{\text{yw}} = 2$, and $\alpha^* = 0.9$. For the lowest sampling rate ($ss = 100$), all the optimum SNR filters degenerate to a single tap ($w^*_{\text{sma}} = w^*_{\text{yw}} = 1$ and $\alpha^* = 1$). A similar analysis was done for the PC-based estimator's window size yielding $w^*_{\text{pc}} = 12$, 6, and 6 for the three sampling rates, respectively. The results of the performance evaluation in the next section utilize these optimum parameters.

## V. PERFORMANCE EVALUATION

Table I summarizes the performance of the estimators in terms of the mean, median, and standard deviation of the absolute value of the PSR estimation error. Results are shown for 1518-byte data packets transmitted at the three data rates of 5.5, 24, and 54 Mbps and for three channel sampling rates (1, 1/10, and 1/100). At the highest channel sampling rate, or effectively the slowest time-varying channel, we observe that the PC-based estimator has mean and median errors that are lower than or similar to the SNR-based estimators. However, when the channel is sampled every 10 slots, the roles are reversed, and the SNR-based estimators perform as well or

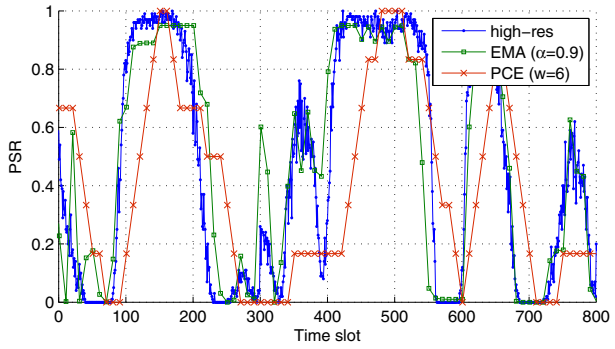


Fig. 6. PSR estimates of PC-based and SNR-based EMA estimators vs. time: sub-sampling interval $ss = 10$, data rate 54 Mbps

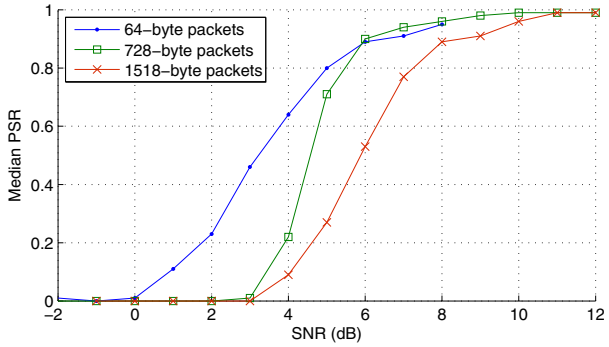


Fig. 7. Median PSR vs. SNR by 5.5 Mbps data packet size

better than the PC-based estimator. At the fastest effective channel speed, the SNR-based estimators are uniformly better. In summary, the SNR-based estimators meet or exceed the accuracy of the PC-based estimator at higher channel speeds and do so with fewer measurements—in most cases a single SNR measurement versus 6 packet counting observations. In fact, the SNR-based estimators at the 1/100 sampling rate are superior to the PC-based estimator at the 1/10 sampling rate. The ability to obtain more accurate estimates with fewer observations translates to lower latency and lower overhead for obtaining an estimate.

Among the SNR-based estimators, there is little difference in performance. While the YW filter generates lower SNR estimation errors in some cases (e.g., Fig 5(a), $ss = 10$), *PSR* estimation error statistics are roughly the same, suggesting that the uncertainty in the SNR-PSR mapping dominates the effect of the filter. The SMA and EMA filters are preferred, therefore, since they require no *a priori* statistical information.

Fig. 6 illustrates the PSR estimates versus time of the PC-based and SNR-based EMA estimators for an 800-slot segment of 54-Mbps transmissions based on rate-1/10 sub-sampling. The latency and coarseness of the length-6 PC-based filter is apparent compared with that of the $\alpha = 0.9$ EMA filter.

Another advantage of the SNR-based schemes is that the same SNR measurements can be used to estimate the PSR of any combination of data rate and packet size, yielding additional overhead savings relative to PC-based estimation. Fig. 7 illustrates empirically-obtained SNR-PSR functions that can be used to estimate the 5.5 Mbps PSR for three different packet sizes: 64, 728, and 1518 bytes.

Finally, a similar analysis as above was performed for a time-varying link in the presence of other 802.11b/g traffic generated by WiFi access points. The results and conclusions were similar as those above, albeit with different SNR-PSR mappings due to the presence of co-channel interference.

## VI. Conclusion

The performance of various estimators of packet success rate on a time-varying link was compared. As the speed of the channel variability increases, packet counting incurs errors due to latency and coarseness of the estimator. SNR-based schemes, which map the current estimated SNR to a PSR value, require fewer measurements and are better able to keep up with temporal changes. A requirement of the SNR-based estimators, however, is a pre-defined function mapping the estimated SNR to a PSR value. Such mappings can be obtained from theoretical or empirical models. With the proper mappings, the same SNR estimate can be used to predict the PSR for various data rates and packet sizes. Simple moving average, exponential moving average, and Yule-Walker predictor filters for estimating the current SNR were tested, and all three performed comparably in terms of PSR estimation, suggesting the error was dominated by the SNR-to-PSR mapping. These conclusions are based on experiments conducted with IEEE 802.11b/g radios and a programmable linear positioner used to induce fine-grained variability in received signal strength.

## References

[1] D. S. J. De Couto, D. Aguayo, J. Bicket, and R. Morris, "A high-throughput path metric for multi-hop wireless routing," in *Proc. ACM MobiCom*, 2003, pp. 134–146.

[2] R. Draves, J. Padhye, and B. Zill, "Routing in multi-radio, multi-hop wireless mesh networks," in *Proc. ACM MobiCom*, 2004, pp. 114–128.

[3] "IEEE P802.11s/D2.0 draft mesh networking amendment," New York: IEEE, 2008.

[4] D. Qiao and S. Choi, "Fast-responsive link adaptation for IEEE 802.11 WLANs," in *Proc. ICC*, vol. 5, May 2005, pp. 3583–3588.

[5] M. R. Souryal, J. Geissbuehler, L. E. Miller, and N. Moayeri, "Real-time deployment of multihop relays for range extension," in *Proc. ACM MobiSys*, Jun. 2007, pp. 85–98.

[6] K.-H. Kim and K. G. Shin, "On accurate measurement of link quality in multi-hop wireless mesh networks," in *Proc. ACM MobiCom*, 2006, pp. 38–49.

[7] D. Aguayo, J. Bicket, S. Biswas, G. Judd, and R. Morris, "Link-level measurements from an 802.11b mesh network," in *Proc. ACM Special Interest Group on Data Communication (SIGCOMM)*, 2004, pp. 121–132.

[8] M. R. Souryal, L. Klein-Berndt, L. E. Miller, and N. Moayeri, "Link assessment in an indoor 802.11 network," in *Proc. IEEE Wireless Communications and Networking Conference (WCNC)*, Apr. 2006.

[9] M. Senel, K. Chintalapudi, D. Lal, A. Keshavarzian, and E. J. Coyle, "A Kalman filter based link quality estimation scheme for wireless sensor networks," in *Proc. IEEE GLOBECOM*, Nov. 2007, pp. 875–880.

[10] Y. Ma, Y. Yu, G.-H. Lu, and Z.-L. Zhang, "Improving wireless link delivery ratio classification with packet SNR," in *Proc. IEEE Int. Conference on Electro Information Technology*, May 2005.

[11] A. Tønnesen, T. Lopatic, H. Gredler, B. Petrovitsch, A. Kaplan, S.-O. Tücke *et al.*, "olsrd: an adhoc wireless mesh routing daemon," Available online at http://www.olsr.org/.

[12] A. Leon-Garcia, *Probability and Random Processes for Electrical Engineering*. 2nd ed., New York: Addison-Wesley Publishing Company, 1994.